Dynamic Monte Carlo simulation of oscillations and pattern formation during the NO + CO reaction on the Pt(1 0 0) surface

S.J. Alas [a], F. Rojas [a], I. Kornhauser [a], G. Zgrablich [b],*

[a] *Departamento de Química, Universidad Autónoma Metropolitana, Iztapalapa, P.O. Box 55-534, México, D.F., México*
[b] *Laboratorio de Ciencias de Superficies y Medios Porosos, Universidad Nacional de San Luis, 5700 San Luis, Argentina*

Abstract

Theoretical simulations by a dynamic Monte Carlo method were carried out with respect to the catalytic reduction of NO by CO on the Pt(1 0 0) surface. This reaction, when occurring at low pressures and under certain reaction conditions, exhibits different temporal and spatiotemporal behaviors, caused by an adsorbate-induced surface restructuring. The studies herein developed take into account recent experimental evidences concerning the NO + CO reaction on the Rh(1 1 1) surface; such experiments have shown that the production of molecular nitrogen occurs preferentially via the formation of an $(N–NO)^*$ intermediary species rather than through the conventional $N + N$ recombination step. Sustained, irregular or damped oscillations as well as the formation of cellular structures and turbulent patterns are observed during our Monte Carlo surface reaction analysis.
© 2005 Elsevier B.V. All rights reserved.

Keywords: NO reduction; Kinetic oscillations; Reaction pattern formation; Surface reconstruction; Dynamic Monte Carlo simulation

1. Introduction

The catalytic reduction of NO by CO proceeds according to the overall reaction:

$$NO + CO \rightarrow CO_2 + (1/2)N_2$$
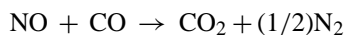
During the past two decades this reaction has deserved a good deal of attention by research workers from both experimental and theoretical points of view [1–14], given that the understanding of this reaction is crucial to help solving the problem of atmospheric pollution by automobile exhausts and industrial gas effluence. The understanding at a molecular level of this reaction on metallic surfaces, in addition to its importance for the development of more efficient catalysts for controlling part of the air pollution, has an intrinsic fundamental interest, due to the fact that interesting non-linear phenomena are involved giving rise to complex behaviors such as kinetic oscillations and spatiotemporal patterns formation.
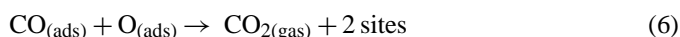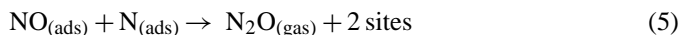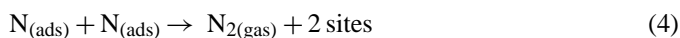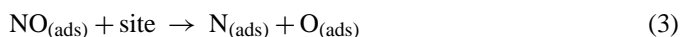
A variety of catalyzed reactions have been found to show oscillatory behavior under nearly real conditions, i.e. polycrystalline surfaces or supported catalysts at relatively high pressures [5]. Under these conditions, reactions are typically non-isothermal and many effects contribute to obscure the delicate interplay of elementary steps conducting to a complex behavior. Experimental studies of catalytic reactions on single crystals in isothermal conditions at low pressures have provided valuable information that can be used to develop and evaluate theoretical models based on the microscopic properties of the system. However, these studies have been concerned with only a narrow range of catalytic reactions, mainly CO oxidation on Pt and Pd surfaces and NO reduction by several agents (CO, H_2 and NH_3) on Pt(1 0 0) and Rh(1 1 0) [5]. It is well known that the (1 0 0) and (1 1 0) faces of noble metals undergo a surface reconstruction driven by adsorbed molecules during these reactions, and this phenomenon is an important ingredient in building up of the oscillatory behavior.

Oscillations and spatiotemporal patterns have particularly been observed for the NO + CO reaction on the Pt(1 0 0) surface under isothermal, low pressure conditions ($p \sim 10^{-6}$ to 10^{-4} Pa) [1–6]. It is well known that the clean Pt(1 0 0) surface at $T > 420$ K exhibits a quasi-hexagonal configuration (hex)

* Corresponding author. Tel.: +54 2652 436151; fax: +54 2652 430224.
E-mail address: giorgio@unsl.edu.ar (G. Zgrablich).

of the atoms in the topmost layer, but surface reconstruction can take place reversibly by the uptake of adsorbates such as CO and NO then leading to the formation of a (1 × 1) square structure [2–8]. This constitutes an adsorbate-induced hex $\rightleftarrows$ 1 × 1 surface phase transition, which, at $T > 450$ K, is directly involved in the formation of oscillations during the course of the NO + CO reaction [2–11]. Another fundamental ingredient, necessary for the observation of kinetic oscillations and spatiotemporal patterns, is a synchronization mechanism, such that the contributions of different local oscillators do not average out to a stationary reaction rate. In controlled isothermal and low pressure conditions the mechanism conducting to this synchronization is the surface diffusion of reactants. A relatively fast surface diffusion of some of the reactants is necessary in order to correlate what is going on in the reaction at relatively distant surface positions.

The typical mechanism of NO reduction by CO on the Pt(1 0 0) surface that has been traditionally assumed in the literature consists of the following sequence of reaction steps:

$$CO_{(gas)} + site \rightleftarrows CO_{(ads)} \tag{1}$$

$$NO_{(gas)} + site \rightleftarrows NO_{(ads)} \tag{2}$$

$$NO_{(ads)} + site \rightarrow N_{(ads)} + O_{(ads)} \tag{3}$$

$$N_{(ads)} + N_{(ads)} \rightarrow N_{2(gas)} + 2\ sites \tag{4}$$

$$NO_{(ads)} + N_{(ads)} \rightarrow N_2O_{(gas)} + 2\ sites \tag{5}$$

$$CO_{(ads)} + O_{(ads)} \rightarrow CO_{2(gas)} + 2\ sites \tag{6}$$

In one of these reaction steps, we can observe that the production of $N_{2(gas)}$ occurs through the recombination of two N atoms adsorbed at two nearest-neighbor sites. The formation of the products of this reaction is directly related to the rate of NO dissociation; moreover, such dissociation can only be performed on the square 1 × 1 phase, since it is quite insignificant on the hex phase of the Pt(1 0 0) surface, as it has been reported in previous studies [4,6,10].

The above reaction mechanism has also been accepted for the same reaction taking place over the Rh(1 1 1) surface [15]. Nevertheless, recent molecular beam studies on this surface carried out by Zaera et al. at $T = 480$ K, have indicated that the standard reaction scheme needs to be modified at least in one of its reaction steps [16–21]. It was found by these researchers that when a ^{14}N-covered Rh(1 1 1) surface is exposed to a ^{15}NO + CO beam, the molecular nitrogen that is being released always contains at least one ^{15}N atom; in this way, the adsorbed ^{14}N molecules are removed exclusively as ^{14}N^{15}N, since ^{14}N^{14}N species were not detected in those experiments [16,17]. This experimental finding means that the adsorbed nitrogen recombination (step (4)), which is usually assumed as responsible of the formation of molecular nitrogen, is in fact not fast enough to account for such production under typical reaction conditions. Instead, an intermediate species is being formed via the interaction of adsorbed atomic nitrogen with undissociated adsorbed NO molecules. The resulting (N–NO)* activated complex may then either decompose to $N_{2(gas)} + O_{(ads)}$ or may simply be desorbed as N$_2$O.

It has already been suggested [22] that the new reaction mechanism observed for Rh(1 1 1) could be valid also for other surfaces like, for example, Rh(1 0 0) or Pt(1 0 0) where the hex $\rightleftarrows$ 1 × 1 phase reconstruction takes place. Although there is no direct experimental evidence for the occurrence of this mechanism on Pt(1 0 0) or Rh(1 0 0), it is also true that there is no direct experimental evidence for the contrary. The production of N$_2$ via a parallel NO + N recombination step has been considered by several authors in the literature. For example, Kortlüke and Von Niessen [23] assume the recombination step in studying the reaction on polycrystalline Rh; Cho [24] proposed a mechanism where N$_2$ is produced via the formation of a surface N$_2$O species, whose formation was demonstrated by early studies for Rh supported on silica [25].

Since the slow step of the catalyzed NO + CO reaction is NO dissociation, the possibility of N$_2$ production through the formation of the (N–NO)* intermediary, instead of the classical N + N recombination, should produce relevant differences in the conditions under which sustained oscillations and patterns formation appear. It is our purpose here to determine these conditions.
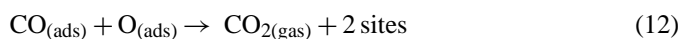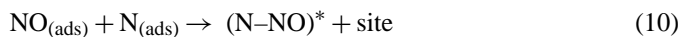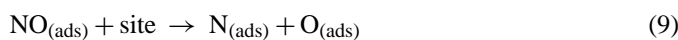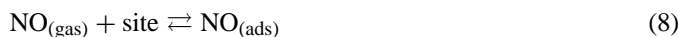
The effects of the modified reaction mechanism on the oscillatory behavior of the catalyzed reaction on Pt(1 0 0) have already been studied in reference [22]. However, for the sake of simplicity, it was assumed in that study that NO adsorption, desorption and NO diffusion processes only took place on the 1 × 1 phase. Even though this could be a reasonable simplifying assumption, based on the fact that NO dissociation takes place significantly only on that phase, NO does certainly adsorb molecularly and diffuse also on the hex phase [26]. This contributes both to the hex $\rightleftarrows$ 1 × 1 phase reconstruction and to the NO mobility, which is very important in view of establishing the synchronization mechanism under the modified reaction mechanism. It is therefore imperative to extend the previous study [22] by allowing NO adsorption, desorption and diffusion processes also on the hex phase, which is the purpose of the present work.

Dynamic Monte Carlo simulations, from which the behavior of the catalytic system can be simulated in real time units [27], will be used in the calculations. Specifically, we will apply the above dynamic simulation technique to the NO + CO reaction on a Pt(1 0 0) surface by considering alternative steps in the reaction mechanism which take into account the experimental findings of Zaera et al. We will discuss under which conditions a series of different oscillatory and spatiotemporal behaviors can be observed and identify which are the dominant physicochemical processes that determine the occurrence of such dynamic patterns. In Section 2, the model and simulation method are described. Results are presented and discussed in Section 3. Finally, conclusions are given in Section 4.

2. Model and simulation method

For the dynamic analysis of the reduction of NO by CO on a Pt(1 0 0) surface, the following general reaction scheme, which includes the new alternative steps according to recent experimental evidence found with respect to the same reaction on the

Rh(1 1 1) surface [20], is assumed:

$$CO_{(gas)} + site \rightleftarrows CO_{(ads)} \tag{7}$$

$$NO_{(gas)} + site \rightleftarrows NO_{(ads)} \tag{8}$$

$$NO_{(ads)} + site \rightarrow N_{(ads)} + O_{(ads)} \tag{9}$$

$$NO_{(ads)} + N_{(ads)} \rightarrow (N–NO)^* + site \tag{10}$$

$$(N–NO)^* \rightarrow N_{2(gas)} + O_{(ads)} \tag{11}$$

$$CO_{(ads)} + O_{(ads)} \rightarrow CO_{2(gas)} + 2\,sites \tag{12}$$

Here $(N–NO)^*$ is the activated complex intermediate, which eventually decays mainly to N_2. In this reaction scheme, it can be observed that we have substituted the conventional $N + N$ recombination step for the production of N_2 by an alternative step involving the formation of the $(N–NO)^*$ species. In addition to the above reaction mechanism we also consider that diffusion of adsorbed NO and CO species can take place on any of the two substrate phases, although not across them. It is important to stress that NO dissociation can only take place on the 1×1 phase, while all other processes can take place on both the hex and the 1×1 phases.

In order to count with a relatively simple and manageable reaction scheme, we incorporate the following additional assumptions in devising our surface reaction mechanism:

(i) The production of N_2O is not taken into account given that the rate of this reaction is expected to be low compared to that corresponding to N_2 production [2].

(ii) The difference in densities between Pt atoms in the hexagonal and in the 1×1 phases is ignored, in spite of the fact that the Pt(1 0 0) surface presents different site densities for the hexagonal and the 1×1 phases, the difference being approximately of 20% [6].

(iii) Lateral interactions among different ad-species occurring on both phases are not considered, even if these effects have been made evident by experimental studies [28,29].

(iv) O_2 desorption is neglected since experiments have shown that this process occurs at temperatures above 600 K [29,30]; in our simulations a temperature of 485 K is kept fixed.

(v) Oxygen diffusion does not occur as this process is expected to be slower if compared to the remaining reaction steps, since the oxygen atoms are strongly bonded to the surface.

(vi) N diffusion is neglected in view that in our reaction scheme N_2 is produced through the formation of an $(N–NO)^*$ intermediary and that both NO desorption and diffusion are allowed. Hence, N and NO species can easily meet at two nearest-neighbor (NN) cells (in contrast, in the classical reaction scheme where N_2 is formed through the recombination of two adsorbed N atoms, N diffusion is strictly required [8,11]).

Our simulation procedure is based on the HS model, which was originally proposed by Gelten et al. for the oxidation of CO by O_2 on a Pt(1 0 0) surface [31]. We believe that this method is suitable for our present study given that CO reduction by NO is similar to CO oxidation, with the only differences that in the former reaction we have more adsorbed species and that NO adsorption needs only one vacant site, dissociation occurring in a later step, while O_2 adsorption and dissociation occurs simultaneously needing two NN vacant sites. This important difference in the particles-vacancies stoichiometry leads, however, to quite different behaviors in the kinetics of the two reactions.

Accordingly, the Pt(1 0 0) surface is represented as a regular 2D grid with periodic boundary conditions. The grid consists of $L \times L$ cells, the state of each cell is described by two labels: label 1 identifies the type of molecule or atom that is adsorbed on that cell, it can also represent an empty cell, while label 2 corresponds to the presence of either the hexagonal (H) or the square (S) phases in that cell. In the square phase, each cell has four neighbors and in the hexagonal phase each cell has six neighbors. There are different (label1:label2) combinations to indicate the condition of each cell and therefore the processes that can occur on it, for instance: (H:H) indicates an empty cell in the hex phase; (X:H) an X species (X = NO, CO, N, O) adsorbed on a cell in the hex phase; (S:S) an empty cell in the 1×1 phase; (X:S) an X species adsorbed on a cell in the 1×1 phase. Other details concerning the HS model can be found in reference [31].

In our model, the time evolution of the system is assumed to occur as a Markovian stochastic process. Under such scheme, every elementary reaction step has a rate constant associated with the probability per unit time for the occurrence of such step. A master equation describes the time evolution of the probability distribution of the states of the physical systems [32]:

$$\frac{\partial P_\alpha(t)}{\partial t} = \sum_\beta [W_{\beta \rightarrow \alpha} P_\beta(t) - W_{\alpha \rightarrow \beta} P_\alpha(t)] \tag{13}$$

Here $P_\alpha(t)$ is the probability to find the system in a given configuration α at time t, it can be considered as a component of a vector P representing the probability distribution of the whole set of system configurations, and W is the transition probability per unit time of the different processes indicated as a subscript.

This master equation can be solved through different methods [33] only in very simple situations. In the case of the reaction considered here, it must be solved through a dynamic Monte Carlo simulation in order to avoid mean field approximations. The simulation can be performed through the "random selection method", which, as adapted to our system, is as follows: (i) a surface cell is selected at random with probability $1/N$; where N indicates the total number of cells existing at the moment; (ii) a given i-type reaction step (i.e. adsorption, desorption, diffusion, etc.) is chosen at random with probability W_i/R, where R is the sum of the rates of all possible processes, i.e. the total-transition rate constant of the system; (iii) if the selected i-type reaction step is viable (according to certain rules to be specified below) on the chosen cell, then it is immediately executed, and (iv) after a given cell is selected, the time is increased by Δt according to

$$\Delta t = -\frac{\ln \xi}{NR} \tag{14}$$

Table 1
Values of the parameters used in simulations and their comparison with their experimentally observed values

Reaction	p^{exp} (Pa)	p^{sim} (Pa)	S_0^{exp}	S_0^{sim}	References
CO adsorption	4×10^{-4}	3.9×10^{-4}	≈ 0.8	0.8	[4,23,32]
NO adsorption	4×10^{-4}	4×10^{-4}	≈ 0.8	0.8	[4,23]
Reaction	ν^{exp} (s^{-1})	ν^{sim} (s^{-1})	E_a^{exp}(kJ/mol)	E_a^{sim}(kJ/mol)	References
CO desorption	4×10^{12} to 1×10^{15}	1×10^{11} to 1×10^{13}	115–157	151–160.5	[6,10]
NO desorption	1.7×10^{14} to 10^{15}	1×10^{11} to 1×10^{13}	142–155	151–160.5	[6,10]
NO dissociation	1×10^{15} to 2×10^{16}	1×10^{15}	117–134	125–139	[6,10]
N$_2$ production	1.3×10^{11}	1×10^{11}	84.6	90	[10]
CO$_2$ production	2×10^{8} to 10^{10}	2×10^{10}	50–100	83.5	[6,10,28]
$1 \times 1 \rightarrow$ hex	2.5×10^{10} to 10^{11}	3×10^{10} to 1×10^{11}	103–107	102–106.5	[6,10,33]
CO nucleation	–	0.015–0.03	≈ 0	0	[28,33–36]
CO trapping	–	0.015–0.03	≈ 0	0	[26,28,36]
CO diffusion	–	0–100	–	–	[28]
NO diffusion	–	0–100	–	–	[22]

where ξ is a random number selected according to a uniform probability in the interval (0,1). This equation renders the real time evolution caused by a system transition.

The following elementary reaction steps and their corresponding rate constants, with the parameter values given in Table 1, are going to be considered.

2.1. Adsorption

The impinging flux of molecules of species i from the gas phase onto the surface is given by

$$J_i = \frac{p_i}{(2\pi m_i kT)^{1/2}} \tag{15}$$

where J_i is the flux of NO or CO molecules per square meter and per second, p_i the partial pressure, m_i the mass of NO or CO, k the Boltzmann constant and T is the absolute temperature. The adsorption rate W_i of particles impinging on the surface per site and per second is then obtained as

$$W_i = J_i A S_0 \tag{16}$$

where A is the number of sites per square meter of surface, in this case of Pt(1 0 0), and S_0 is the initial sticking coefficient. CO and NO can be adsorbed on both the hex and the 1×1 phase.

2.2. Desorption

Desorption is considered as an activated process with a rate given by

$$W_i = \nu_i \exp\left(-\frac{E_{ai}}{kT}\right) \tag{17}$$

where ν_i is the frequency factor and E_{ai} the activation energy for species i.

CO and NO desorption occurs both from the hexagonal and 1×1 phases at the same rate; actually, experiments indicate that these rates may be different [6,10].

2.3. Diffusion

Diffusion jumps are allowed both for CO and NO species to vacant NN cells. These jumps can be performed on any of the two phases but not across the interface between them. The diffusion rate W_i is obtained directly as a frequency factor ν_i.

2.4. NO dissociation

On a Pt(1 0 0) surface this process can only occur on the 1×1 phase and with the availability of a NN vacant cell. The dissociation rate is calculated as an activated process, as in Eq. (17), with appropriate frequency factor and activation energy.

2.5. N$_2$ production

This reaction is possible whenever the formation of an intermediate (see reaction scheme steps (10) and (11)) (N–NO)* species takes place. This is considered as an activated process, with appropriate frequency factor and activation energy, and occurs rapidly according to experimental observations [10] if a pair of NN cells is occupied by N and NO species. This reaction can take place across phase boundaries.

2.6. CO$_2$ production

This process is possible when two NN cells are occupied by CO and O species. It is considered as an activated process and can take place across phase boundaries.

2.7. Surface reconstruction

Experimental results indicate that the hex $\rightarrow 1 \times 1$ phase transition occurs by nucleation and trapping of the CO molecules on the Pt(1 0 0) surface, a similar mechanism is assumed here for adsorbed NO; this transformation of the surface is caused by the different heats of adsorption of these two species on both phases [28,36–38], which is considerably higher on the unreconstructed 1×1 phase than on the reconstructed hexagonal one [26]. The

observations show that four to five molecules are involved in the restructuring process [35]. Thiel et al. proposed that this transformation occurs by a sequential mechanism: initially, the 1×1 phase is formed by nucleation of adsorbed molecules on a precursory hexagonal phase, this is followed by the migration and trapping of the molecules by way of growing islands [39].

Incorporating these experimental results into our model, we assume the following two mechanisms: (i) the *nucleation* mechanism for the hex $\rightarrow 1 \times 1$ reconstruction takes place if there exist five adsorbed molecules (CO, NO or a mixture of both) forming a nucleating cluster; (ii) island growth on the square phase happens through a *trapping* mechanism, i.e. when a molecule on the hexagonal phase is in a NN position to a molecule belonging to a reconstructed 1×1 island then it is trapped into that island and its cell reconstructs from the hexagonal to the square phase. The fact that a growing island can be made by CO and NO is based on experimental evidence establishing that the heats of adsorption of both molecules are almost the same [26]. The rates for these two processes are determined directly by appropriate frequency factors.

The inverse $1 \times 1 \rightarrow$ hex transformation occurs in empty cells of the square phase. In this analysis, we only require of a cell to perform this transformation, which is considered as an activated process with appropriate frequency factor and activation energy [6,10,36].

3. Results and discussion

In the simulations performed in this work, both the partial pressures of reactants in the gas phase as well as the system temperature are kept constant. Experimentally, the NO reduction by CO on the Pt(1 0 0) crystal face displays sustained and damped oscillations in the temperature range 478–490 K and at NO and CO partial pressures of about 10^{-4} Pa [4]. The temperature selected for our analysis was 485 K and the partial pressures of NO and CO were chosen as 4×10^{-4} and 3.87×10^{-4} Pa, respectively.

The principal results of the CO + NO reaction simulation study will be now presented, afterward, a discussion concerning the effect that each reaction step or surface process can produce on the behavior of the system will be undertaken. For the sake of simplicity, some of the reaction parameters will not be specifically mentioned throughout this discussion, since these quantities are thought to have little influence on the development of the different kinetic oscillation types and on the formation of assorted surface patterns. Table 1 shows the values of the parameters that have been employed in our simulations in order to obtain the rate of each elementary reaction step; experimental values of these parameters are also included for comparison. In view that no available data account for the decay of the $(N–NO)^*$ complex intermediary to N_2 and consequently for the value of corresponding rate constant, we have instead employed for this assignment the experimental values of N_2 formation proceeding from the classical N + N recombination.

According to the experimental data about the reduction of NO by CO on the Pt(1 0 0) face, sustained rate oscillations can occur at elevated temperature ($T > 478$ K). Under such circumstances, the oscillations are due to the hex $\rightleftarrows 1 \times 1$ phase transition; the appearance of these temporal patterns has been explained through the formation of a synchronized phase transition mechanism [3,4]. Nevertheless, at lower temperatures the oscillatory behavior can be observed on a local scale on a homogeneous 1×1 substrate without the involvement of the hex $\rightleftarrows 1 \times 1$ phase reconstruction, in this case there is no synchronized mechanism and no sustained rate oscillations exist [4]. In our study, corresponding to the higher temperature region, the appearance of sustained oscillations is possible by means of the development of a synchronized hex $\rightleftarrows 1 \times 1$ phase transition mechanism. Moreover, sustained oscillations are usually associated to the formation of cellular structures. This synchronized mechanism can be explained as follows.

The simulation of the NO + CO reaction on the Pt(1 0 0) surface starts from a completely hex-reconstructed clean surface, on which it is feasible to observe the adsorption of both CO and NO molecules. At a certain surface coverage value, small nuclei of CO, NO or CO/NO mixtures can be formed on the surface according to certain probability values; these clusters can then transform small surface regions from the hex to the square phase thus forming 1×1-CO, 1×1-NO and 1×1-CO/NO islands. Afterward, these nuclei can grow by trapping reactions; this part of the evolution of the system is known as the *transformation stage*. The growth of these islands is a stable process, since the reaction can be locally inhibited by a relatively high adsorbate coverage, which hinders the NO dissociation. However, when either a CO or NO molecule desorbs from the square phase surface toward the gas phase, an empty cell appears and, if this vacancy has a NN adsorbed NO molecule, then this NO molecule has the possibility of dissociating into N and O atoms. Now, it is pertinent to mention that the 1×1 phase is the one that is active during NO dissociation, while the hex phase is ineffective at this respect. If this dissociation step is accomplished, the adsorbed oxygen atom can then react with a CO adsorbed molecule while, in turn, the N adsorbed atom can also react with a NO adsorbed molecule thus forming the $(N–NO)^*$ complex intermediate. The species that are formed on the surface can desorb as CO_2 and N_2 into the gas phase. So that, new vacant cells can be formed on the 1×1 phase by allowing more NO adsorbed molecules to dissociate; subsequently, more O and N atoms can continue reacting, leading to an autocatalytic "explosive" reaction. In this way, a reaction front starts to propagate across the surface. As a result of this process, a *reactive stage* is developed on the 1×1 phase. As vacant cells existing on the square phase have a finite probability to undergo the $1 \times 1 \rightarrow$ hex reconstruction, then small areas of the surface can slowly return to the hexagonal configuration. This last process is known as the *recovery stage*, in this way the reactive stage is gradually extinguished. CO, NO and CO/NO nuclei will be formed once more and the oscillatory cycle will resume again from the transformation stage. Gelten et al. proposed a similar synchronized mechanism in their simulation model related to CO oxidation on Pt(1 0 0) [31].

The above scenario is depicted in Figs. 1 and 2. In Fig. 1, we can observe sustained oscillations obtained from a simulation performed on a lattice with 1024×1024 cells. In Fig. 1(a), it
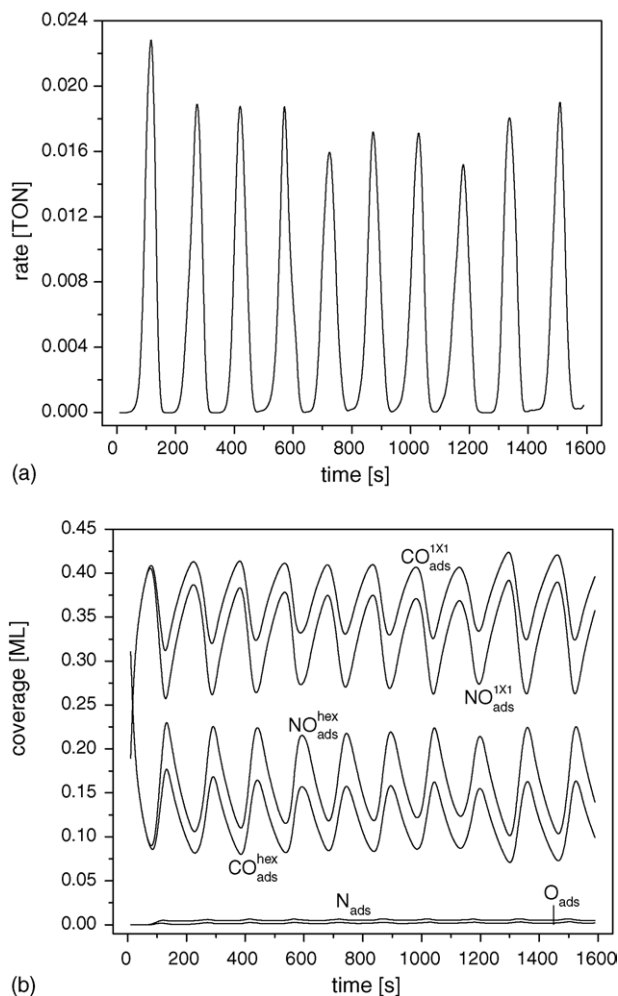
Fig. 1. Sustained oscillations: (a) CO_2 production rate in turnover number (TON); (b) coverage of adsorbed CO and NO molecules on hexagonal and square phases (N and O coverage values are also indicated). Rates for $W_{COdes} = W_{NOdes} \approx 5 \times 10^{-7} \, s^{-1}$, $W_{COdif} = 100 \, s^{-1}$, $W_{NOdif} = 0 \, s^{-1}$, $W_{H \to S} = 0.015 \, s^{-1}$, $W_{S \to H} \approx 0.5 \, s^{-1}$, $W_{NOdis} \approx 1 \, s^{-1}$. Grid size: 1024×1024 cells.

is possible to visualize the rate of production of CO_2 measured as turn over number (TON), i.e. the number of CO_2 molecules produced per Pt atom per second. Fig. 1(b) shows the surface coverage of each adsorbed species measured in monolayers (ML). Fig. 2 shows the formation of cellular patterns, i.e. snapshots of the surface evidencing the existence of the synchronized mechanism: Fig. 2(a) depicts the *transformation stage* at 200 s; Fig. 2(b) represents the *reactive stage* at 240 s, here we can clearly see the formation of reaction fronts spreading across the surface; Fig. 2(c) shows that when these fronts grow sufficiently in size then they start to collide against each other at a time of 265 s; and Fig. 2(d) shows how these reaction fronts extinguish at a time of 280 s. Analogous reaction fronts and its subsequent propagation were reported by Tammaro and Evans for the NO + CO reaction on a Pt(1 0 0) surface via reaction–diffusion equations [13]. Experimentally these cellular patterns have been observed for the $CO + O_2$ reaction taking place on a Pt(1 1 0) surface [34].

We have found in this work, that CO and NO surface diffusion processes are very important in the behavior of the system. When these diffusion processes are incorporated or excluded, the following phenomena have been observed:

(a) When the rate of CO diffusion is relatively high (i.e. $50 \, s^{-1}$) and when the rate of NO diffusion is neglected, sustained oscillations can be obtained. This can be explained in view of the relatively high CO diffusion rate, which induces CO molecules to move on both (hexagonal and square) surface phases. Besides, CO and CO/NO mixture nuclei are formed slowly and thereby the hex $\to 1 \times 1$ transformation is slow too. In this way, most of the nuclei will be constituted by NO. Consequently, NO desorption is more probable to occur than CO desorption, thus generating some empty cells and hence the possibility that a NO molecule can dissociate into N and O atoms then starting the propagation of reaction fronts across the 1×1 phase. Due to the high CO mobility, the probability of reaction between CO and oxygen is high. On large grids (512×512 and 1024×1024 cells) reaction fronts are created; these fronts collide and are extinguished against each other (see Fig. 2). However, if the CO diffusion rate decreases by some reason, then the oscillation periods become longer. This happens as a consequence of the fact that, due to a slower mobility of CO molecules, the reaction between CO molecules and O atoms is delayed. This behavior is shown in Fig. 3. On the other hand, if the CO diffusion rate is increased, the oscillation period is shorter due to the increase of the probability of the reaction $CO_{(ads)} + O_{(ads)}$ produced by the higher CO mobility. But if this diffusion rate continues to be increased, the sustained oscillations start to decay into irregular and damped oscillations, since too many reaction fronts are created on the surface and collide against each other, although these fronts do not lead to complete extinction. Remnants of these reaction fronts can still survive when new fronts are generated on the surface; the recovery stage is not observed any more thus spoiling the synchronized oscillatory behavior.

(b) When both CO and NO diffusion rates attain suitable values, the oscillatory behavior is as follows. If NO diffusion rate increases the period of the sustained oscillation becomes shorter. According to these results, we believe that when NO is not moving on the surface, NO molecules act like an impervious wall that interposes between the existing CO molecules and the oxygen atoms. In this way, if NO diffusion is increased, CO molecules have a greater opportunity to find an O atom and to react faster than when NO is not diffusing. For example, if CO and NO diffusion rate constants are the same (e.g. $50 \, s^{-1}$), the oscillation periods are shorter than if CO and NO diffusion rates have values of 5 and $10 \, s^{-1}$ or 10 and $10 \, s^{-1}$, respectively. Now, if the diffusion rates for both molecules are equal to $10 \, s^{-1}$, the oscillation period becomes longer than when CO and NO diffusion rates attain values of 50 and $10 \, s^{-1}$, respectively. In other words, a faster diffusion of both molecules on the surface causes shorter oscillation periods. This result is consistent with the experimentally observed decrease in the
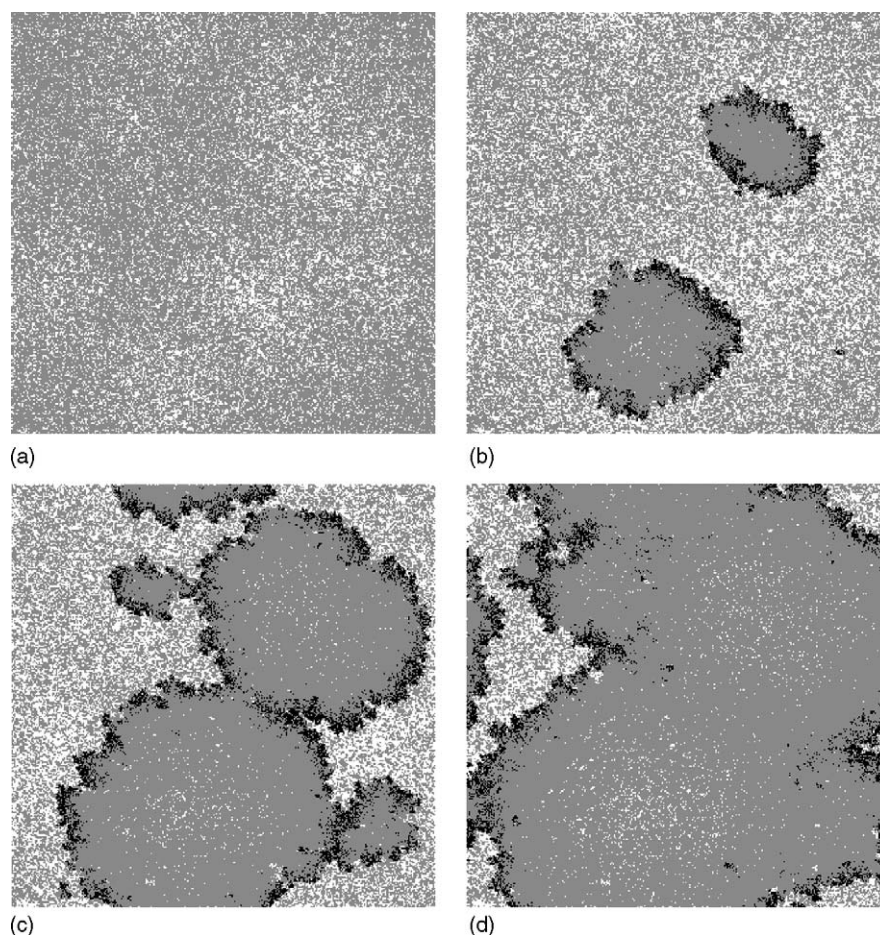
Fig. 2. Snapshots correspond to oscillations of Fig. 1. Grey areas indicate CO/NO on the hexagonal phase, white areas show CO/NO on the 1 × 1 phase and black areas are empty cells on the hexagonal and 1 × 1 phases.

oscillation period when the temperature is slightly increased [6].

(c) When the NO diffusion rate is larger than that of CO, the original sustained oscillations transform into irregular and damped ones. This happens in view of the fact that, if NO

Fig. 3. Effect of CO mobility on sustained oscillations. Thin and thick lines correspond to $W_{CODif} = 100\,s^{-1}$ and $W_{CODif} = 50\,s^{-1}$, respectively. Grid size: 1024 × 1024 cells.

molecules can move faster than CO molecules, when NO dissociation occurs CO molecules are no longer capable of consuming all O atoms and small amounts of oxygen remains on the 1 × 1 phase. This fact can be observed in Fig. 4, in which irregular oscillations can be observed.

(d) When CO diffusion is neglected, oscillations are not observed over a long time since the surface is slowly poisoned by O atoms on the square phase.

It can also be noted that CO and NO desorption processes are the most important promoters for the formation of reaction fronts. If these desorption processes are neglected, the oscillatory behavior can never be produced and the 1 × 1 phase will eventually become poisoned with CO and NO molecules. In consequence, either CO or NO desorption would trigger oscillations. In our simulation, sustained oscillations are obtained if the rate constants for desorption processes are rather low and, as the CO and NO partial pressures are almost the same, the rates of adsorption are expected to be similar for both gases. For these reasons, CO and NO desorption rates are estimated to be about equal for both molecules. If the desorption rate constants of CO and NO are increased, then sustained oscillations will begin to decay into irregular oscillations; if these rates are increased even more, then the irregular oscillations are transformed into
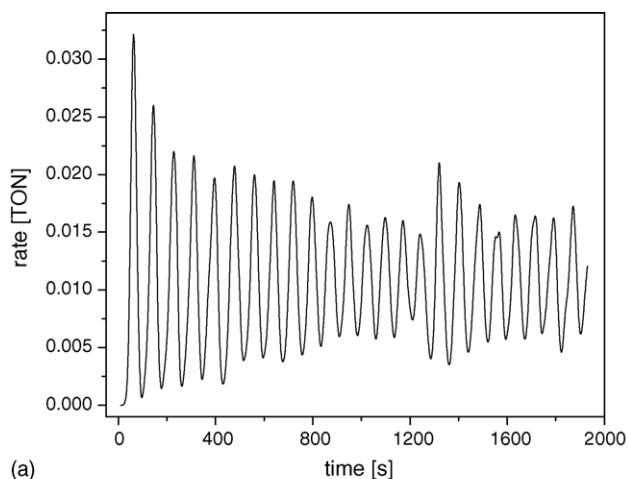
(a)
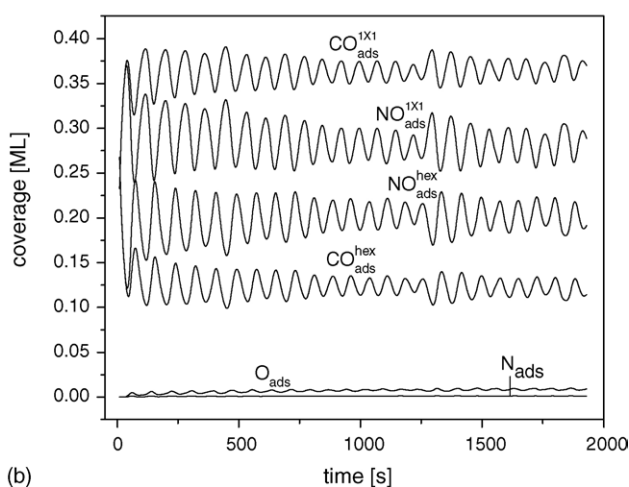
(b)

Fig. 4. Irregular oscillations: (a) CO_2 reaction rate for $W_{COdif} = 10\,s^{-1}$, $W_{NOdif} = 50\,s^{-1}$; (b) coverage of adsorbed CO and NO molecules on hexagonal and square phases (N and O coverage values are also indicated). Other rates are: $W_{COdes} = W_{NOdes} \approx 1 \times 10^{-6}\,s^{-1}$, $W_{H \to S} = 0.022\,s^{-1}$, $W_{S \to H} \approx 0.5\,s^{-1}$, $W_{NOdis} \approx 1\,s^{-1}$. Grid size: 1024×1024 cells.

damped oscillations. This kind of behavior can be understood by considering that desorption and reaction processes compete against each other: if CO and NO desorption rates are too high, then these two species are eliminated from the surface faster than through the reactions producing CO_2 and N_2.

Some other studies were performed in this work such as the influence of transformation rates on the oscillations. The following situations were found:

(i) The model employed here is very susceptible to the hex $\to 1 \times 1$ phase transition. If nucleation and trapping rates have frequency values of $0.015\,s^{-1}$, sustained oscillations can be observed. If these values are increased, the sustained oscillations decay toward damped oscillations. The transformation stage is faster than the recovery stage, since an empty cell that undergo $1 \times 1 \to$ hex phase transition can be occupied by either a CO or NO molecule, which quickly reconstructs toward the square phase by means of trapping or nucleation reactions. Such molecules can be desorbed from the square phase and, if a NO dissociates, a new

reaction front is formed, while the old reaction fronts are not completely extinguished. This breaks down the synchronized mechanism. If the rate constants are decreased, the oscillation periods are longer, the nuclei and the trapping reactions are created slowly on the surface and the transformation stage is deferred.

(ii) On the other hand, when the $1 \times 1 \to$ hex transformation rate attains a value of about $0.5\,s^{-1}$ approximately, sustained oscillations are observed. If this transformation rate is decreased, the sustained patterns decline in favor of a damped behavior; the square phase cannot reconstruct into the hexagonal phase, i.e. the recovery stage does not have enough strength for this to be completed, then destroying the synchronized mechanism. Nevertheless, if this same rate is increased, the oscillation periods become shorter, and if such a rate is increased even more, irregular oscillations are observed.

The most regular and sustainable oscillatory patterns are obtained when the NO dissociation rate constant has a low value
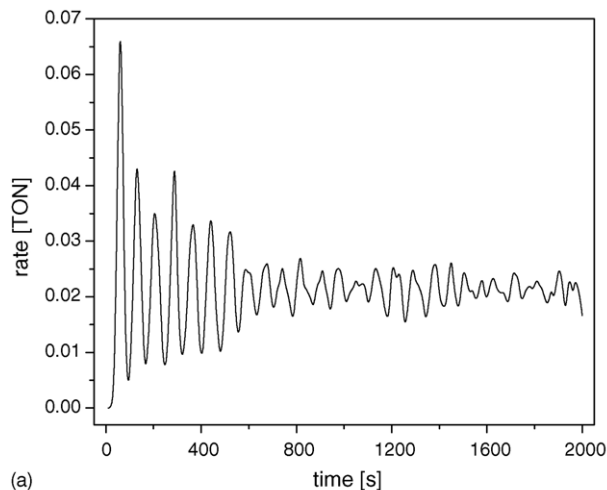
(a)
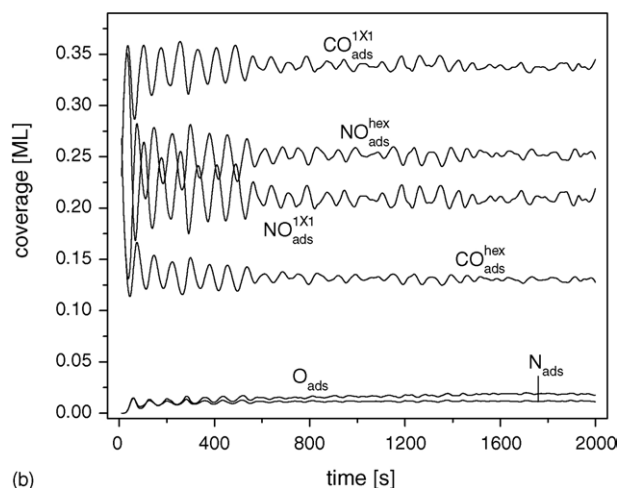
(b)

Fig. 5. Damped oscillations: (a) CO_2 reaction rates for $W_{COdes} = W_{NOdes} \approx 1 \times 10^{-6}\,s^{-1}$, $W_{COdif} = 10\,s^{-1}$, $W_{NOdif} = 0\,s^{-1}$, $W_{H \to S} = 0.022\,s^{-1}$, $W_{S \to H} \approx 0.25\,s^{-1}$, $W_{NOdis} \approx 5\,s^{-1}$; (b) coverage of adsorbed CO and NO molecules on hexagonal and square phases (N and O coverage values are also indicated). Grid size: 1024×1024 cells.
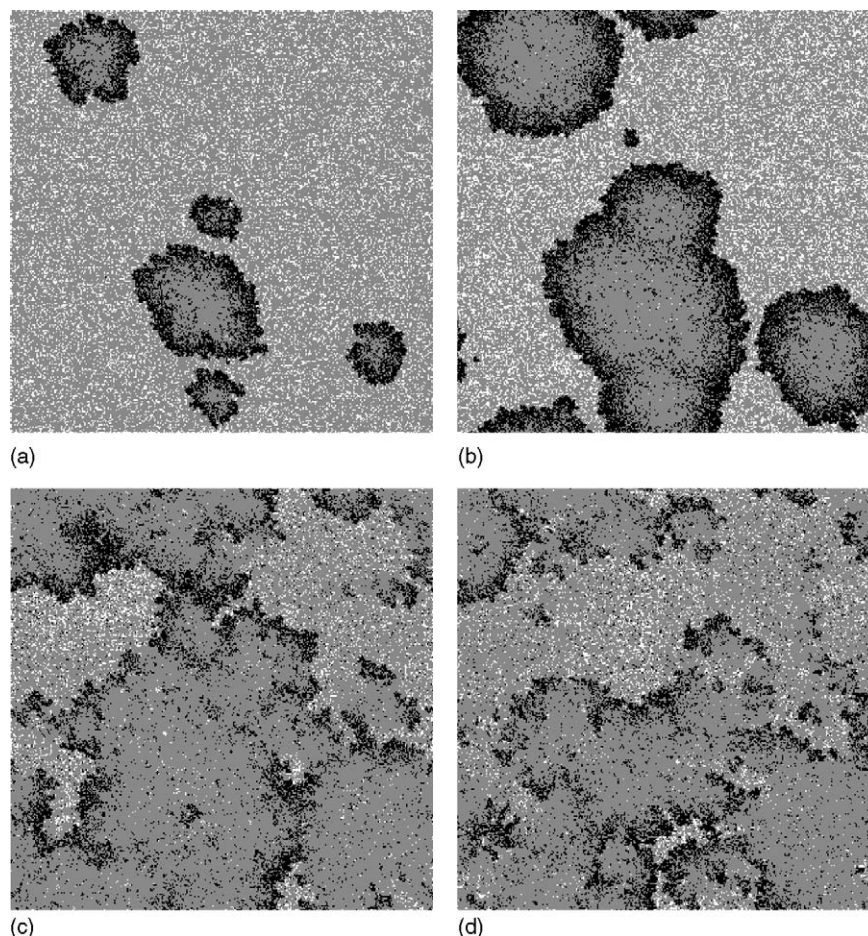
Fig. 6. Patterns formation during a simulation on a grid of 1024×1024 cells: (a) cellular patterns formation at 40 s; (b) growing up of the cellules and collision between them at 50 s; (c) turbulent patterns formation at 130 s; and (d) the turbulent behavior is preserved at 200 s. Grey areas indicate CO/NO on the hexagonal phase, white areas show CO/NO on the 1×1 phase and black areas are empty cells on the hexagonal and 1×1 phases (O and N are also designated with black color).

$(\approx 1\,\text{s}^{-1})$. If this rate is increased, the oscillation periods become shorter, this happens because there exist many O and N atoms on the surface and, if the adsorbed CO or NO molecules have high diffusion rates $(50\,\text{s}^{-1})$, these atoms can then react rapidly to produce CO_2 and N_2. On the other hand, if the diffusion rates of CO or NO are slow $(10\,\text{s}^{-1})$, the sustained oscillations are transformed into damped oscillations since the adsorbed CO or NO molecules are moving slowly on the surface, and cannot completely react with the O and N atoms. Therefore, remnants of O and N atoms can survive on the square phase.

Finally, we have found that when a sustained oscillatory behavior declines in favor of irregular or damped regimes, then the cellular patterns decay into turbulent spatial patterns. The clearest signals of spatiotemporal behaviors are obtained when using large grids, i.e. 512×512 cells or more. In Fig. 5, we can observe a series of damped oscillations. Fig. 6 shows cellular structures and their successive decline into turbulent regimes, these last figures correspond to those of Fig. 5. Turbulent patterns have been observed both experimentally and theoretically [1,4,8]. It is pertinent to mention that on small grids (32×32 and 64×64 cells) oscillations are not very well defined and on intermediate grid sizes (i.e. 128×128 and 256×256 cells) oscillations are produced. In a grid of 256×256 cells, a reaction

front can be readily created: this front can then collide with some others and can be extinguished throughout periodic boundary conditions.

In this study we were not able to find appropriate conditions for the appearance of modulated oscillations like those found in reference [22], where NO were not allowed to adsorb or diffuse on the hex phase. On the other hand we were able to find here bubble patterns, while in the above paper only turbulent patterns were obtained.

It is worth mentioning that, given the relevant progresses being done in studying catalyzed reactions through DFT calculations [40–42], the combination of Monte Carlo simulations and DFT calculations appears as a powerful tool to be used in the future to describe these reactions from a more fundamental point of view.

4. Conclusions

We have studied by dynamic Monte Carlo simulation the oscillatory behavior of the NO + CO reaction on Pt(1 0 0) in the high temperature range under the hypothesis that the main reaction step conducting to the formation of N_2 is not the classical N + N recombination step but the formation of the

(N–NO)[*] intermediary, as suggested by experiments performed on Rh(1 1 1). The principal result of the present study is the appearance of a sustained oscillatory behavior associated with the formation of bubble-like patterns, in contrast to the behavior found with the classical mechanism [8].

The effects of the rates of the main elementary steps, namely CO and NO diffusion and desorption, NO dissociation and phase transformations, on the behavior of the system have been investigated in detail, with the following principal results:

(a) Sustained oscillations can only be observed if a synchronized mechanism is achieved and moreover if cellular spatial patterns are formed. On the other hand, when irregular and damped oscillations are observed, the synchronization is always broken down and cellular structures decline in turbulent spatial behaviors, which are maintained indefinitely.

(b) Such a synchronized mechanism is better achieved and is more stable when the NO dissociation rate is relatively low ($\approx 1\,s^{-1}$) and the diffusion rates of CO and NO are around $50\,s^{-1}$.

(c) CO diffusion is more important than NO diffusion, in fact the latter can be suppressed and still sustained oscillations can be obtained, while no oscillations appear if the former is suppressed. Intermediate values of CO and NO diffusion rates, say between 10 and $50\,s^{-1}$, are adequate for a sustained oscillatory behavior. An increase in these rates produces shorter periods, however irregular and damped oscillations are produced when CO mobility is too high or when NO mobility is higher than that of CO.

(d) CO and NO desorption rates need to be tuned to rather low values for sustained oscillations. Increasing them leads to irregular oscillations, while increasing them further more leads to damped oscillations.

Acknowledgments

References

[1] G. Veser, R. Imbihl, J. Chem. Phys. 96 (1992) 7155.
[2] S.B. Schwartz, L.D. Schmidt, Surf. Sci. 206 (1988) 169.
[3] G. Veser, F. Mertens, A.S. Mikhailov, R. Imbihl, Phys. Rev. Lett. 71 (1993) 935.
[4] G. Veser, R. Imbihl, J. Chem. Phys. 100 (1994) 8483;
    G. Veser, R. Imbihl, J. Chem. Phys. 100 (1994) 8492.
[5] R. Imbihl, G. Ertl, Chem. Rev. (Washington, DC) 95 (1995) 697.
[6] Th. Fink, J.-P. Dath, R. Imbihl, G. Ertl, J. Chem. Phys. 95 (1991) 2109.
[7] N. Khrustova, G. Veser, A. Mikhailov, R. Imbihl, Phys. Rev. Lett. 75 (1995) 3564.
[8] V.P. Zhdanov, J. Chem. Phys. 110 (1999) 8748.
[9] Th. Fink, J.-P. Dath, R. Imbihl, G. Ertl, Surf. Sci. 251 (1991) 985.
[10] Th. Fink, J.-P. Dath, M.R. Bassett, R. Imbihl, G. Ertl, Surf. Sci. 245 (1991) 96.
[11] N. Hartmann, Y. Kevrekidis, R. Imbihl, J. Chem. Phys. 112 (2000) 6795.
[12] B. Meng, W.H. Weinberg, J.W. Evans, J. Chem. Phys. 101 (1994) 3234.
[13] M. Tammaro, J.W. Evans, J. Chem. Phys. 108 (1998) 7795.
[14] O. Kortlüke, V.N. Kuzovkov, W. von Niessen, Phys. Rev. Lett. 81 (1998) 2164.
[15] V.P. Zhdanov, B. Kasemo, Surf. Sci. Rep. 29 (1997) 31.
[16] F. Zaera, C.S. Gopinath, J. Chem. Phys. 111 (1999) 8088.
[17] F. Zaera, C.S. Gopinath, Chem. Phys. Lett. 332 (2000) 209.
[18] C.S. Gopinath, F. Zaera, J. Phys. Chem. B 104 (2000) 3194.
[19] F. Zaera, S. Wehner, C.S. Gopinath, J.L. Sales, V. Gargiulo, G. Zgrablich, J. Phys. Chem. B 105 (2001) 7771.
[20] V. Bustos, C.S. Gopinath, R. Uñac, F. Zaera, G. Zgrablich, J. Chem. Phys. 114 (2001) 10927.
[21] F. Zaera, C.S. Gopinath, J. Chem. Phys. 116 (2002) 1128.
[22] S.J. Alas, S. Cordero, I. Kornhauser, G. Zgrablich, J. Chem. Phys. 122 (2005) 144705.
[23] O. Kortlüke, W. Von Niessen, J. Chem. Phys. 105 (1996) 4764.
[24] B.K. Cho, J. Catal. 138 (1992) 255.
[25] W.C. Hecker, A.T. Bell, J. Catal. 84 (1983) 200.
[26] Y.Y. Yeo, L. Vattuone, D.A. King, J. Chem. Phys. 104 (1996) 3810.
[27] K. Binder, Monte Carlo Methods in Statistical Physics, Springer, Berlin, 1986.
[28] R.J. Behm, P.A. Thiel, P.R. Norton, G. Ertl, J. Chem. Phys. 78 (1983) 7437;
    R.J. Behm, P.A. Thiel, P.R. Norton, G. Ertl, J. Chem. Phys. 78 (1983) 7448.
[29] M.A. Barteau, E.I. Ko, R.J. Madix, Surf. Sci. 102 (1981) 99.
[30] P.R. Norton, K. Griffiths, P.E. Binder, Surf. Sci. 138 (1984) 125.
[31] R.J. Gelten, A.P.J. Jansen, R.A. van Santen, J.J. Lukkien, J.P.L. Segers, P.A.J. Hilbers, J. Chem. Phys. 108 (1998) 5921.
[32] N.G. van, Kampen, Stochastic Processes in Physics and Chemistry, North-Holland, Amsterdam, 1992.
[33] J.J. Lukkien, J.P.L. Segers, P.A.J. Hilbers, R.J. Gelten, A.P.J. Jansen, Phys. Rev. E 58 (1998) 2598;
    H. Hinrichsen, Adv. Phys. 49 (2000) 815.
[34] K.C. Rose, D. Battogtokh, A. Mikhailov, R. Imbihl, W. Engel, A.M. Bradshaw, Phys. Rev. Lett. 76 (1996) 3582.
[35] A. Hopkinson, J.M. Bradley, X.C. Guo, D.A. King, Phys. Rev. Lett. 71 (1993) 1597.
[36] Y.Y. Yeo, C.E. Wartnaby, D.A. King, Science 268 (1995) 1731.
[37] T.E. Jackman, K. Griffiths, J.A. Davies, P.R. Norton, J. Chem. Phys. 79 (1983) 3529.
[38] P.A. Thiel, R.J. Behm, P.R. Norton, G. Ertl, Surf. Sci. 121 (1982) L553.
[39] A. Hopkinson, J.M. Bradley, X.C. Guo, D.A. King, Phys. Rev. Lett. 71 (1993) 1597.
[40] K. Reuter, D. Frenkel, M. Scheffler, Phys. Rev Lett. 93 (2004) 116105.
[41] K. Honkala, A. Hellman, I.N. Remediakis, A. Logadottir, A. Carlsson, S. Dahl, C.H. Christensen, J.K. Norskov, Science 307 (2005) 555.
[42] P. Kamakoti, B.D. Morreale, M.V. Ciocco, B.H. Howard, R.P. Killmeyer, A.V. Cugini, D.S. Sholl, Science 307 (2005) 569.